

Numerical generation of omnistrain failure envelopes

Elalfy, Mohamed H.; Abdalla, Mostafa M.; Abuefoutouh, Nader

DOI

[10.1177/00219983231204948](https://doi.org/10.1177/00219983231204948)

Publication date

2023

Document Version

Final published version

Published in

Journal of Composite Materials

Citation (APA)

Elalfy, M. H., Abdalla, M. M., & Abuefoutouh, N. (2023). Numerical generation of omnistrain failure envelopes. *Journal of Composite Materials*, 57(29), 4603-4614.
<https://doi.org/10.1177/00219983231204948>

Important note

To cite this publication, please use the final published version (if applicable).
Please check the document version above.

Copyright

Other than for strictly personal use, it is not permitted to download, forward or distribute the text or part of it, without the consent of the author(s) and/or copyright holder(s), unless the work is under an open content license such as Creative Commons.

Takedown policy

Please contact us and provide details if you believe this document breaches copyrights.
We will remove access to the work immediately and investigate your claim.

Numerical generation of omnistrain failure envelopes

Mohamed H. Elalfy^{1,2} , Mostafa M. Abdalla³ and
Nader Abuefoutouh⁴

Journal of Composite Materials

2023, Vol. 57(29) 4603–4614

© The Author(s) 2023



Article reuse guidelines:

sagepub.com/journals-permissions

DOI: 10.1177/00219983231204948

journals.sagepub.com/home/jcm

Abstract

Traditional failure criteria for composites are usually formulated in material coordinates and depend on all three inplane stresses, hence failure evaluation depends on the ply angle. The omnistrain failure envelope describes the most critical failure envelope in strain space irrespective of ply orientation. This independence of ply orientation leads to an isotropic failure criterion that depends only on the principal strains. Omnistrain envelopes greatly simplify the task of design and optimisation of composite laminates. This paper proposes a numerical technique to generate omnistrain failure envelopes for different composite failure criteria. The failure index, describing how far a point in strain space is from the failure boundary, is used to describe the failure surface. Assuming convexity of the failure surface, a set of points is generated on the surface, and the convex hull algorithm is used to generate a polygonal approximation of the failure surface. Representing strains in terms of principal strains and the angle between the principal and material coordinates, allows us to eliminate the angle analytically by considering the worst case condition. The omnistrain envelope is thus directly generated from the approximate three-dimensional failure surface. The proposed algorithm does not require analytic expressions of the failure surface. An adaptive algorithm is proposed to generate the omnistrain envelope with relatively small number of points. As demonstration of the proposed algorithm, the omnistrain envelopes for various composite materials are generated for a number of composite failure criteria. The omnistrain envelopes generated for the Tsai-Wu criteria accurately match to existing analytic expressions.

Keywords

Composite failure, omnistrain envelope

Introduction

Strength of conventional Engineering materials such as Aluminum, Copper, Steel etc., can be dealt with as a unique value regardless of loading and dimensions. However, special attention should be given when assessing failure in composite materials, due to their non-homogeneity and anisotropy. Strength properties and failure mechanisms of composite materials, change with the direction of loading which makes the problem more complicated. Many theories have been developed for decades to predict the failure for fiber reinforced composites either in lamina or laminate. A

set of theories, such as maximum stress and maximum strain criteria, are called limit or non-interactive theories, as they predict failure by comparing individual stress or strain components with corresponding strengths or ultimate strains. There is no interaction between stress or strain components. On the other hand, interactive theories predict failure through formulas that include interactions between all stress or strain components but the mode of failure is still undetermined. The most known interactive criteria that are used till now are Tsai-Hill¹ and Tsai-Wu² criteria. The previously mentioned methods did not account for failure

¹Zewail City of Science and Technology, 6th of October City, Egypt

²Currently PhD Candidate, Delft University of Technology, Delft, Netherlands

³Zewail City of Science and Technology, 6th of October City, Egypt

⁴Cairo University, Cairo, Egypt

Corresponding author:

Mohamed H. Elalfy, TU Delft Faculty of Aerospace Engineering, Kluyverweg 1, 2629 HS Delft, The Netherlands.

Email: M.H.I.Elalfy@tudelft.nl

modes for matrix and fiber which is covered by failure-mode-based-theories, where separate criteria are given for each constituent. As an example, Hashin³ proposed to separate matrix failure modes from those of the fiber. For each failure mode or mechanism, tension is distinguished from compression resulting in four distinct failure modes.

Tsai⁴ proposed the omnistrain failure envelope which is defined as the most critical inner failure envelope. This idea facilitates the design of composite materials as the generated envelopes are independent of ply orientations. Tsai and Melo⁵ generated omni strain last ply failure envelopes based on Tsai-Wu and maximum strain failure criteria. They proposed a unit circle failure envelope for any carbon fiber laminate. Furtado et al⁶ predicted the notched strength of carbon/epoxy laminates using invariant-based approach introduced by^{4,5} Millen and Aravand⁷ assessed the unit circle failure envelope and results showed it was conservative in general.

There were attempts in literature to find analytical expressions of the omnistrain envelopes. Analytical expressions of the omnistrain failure envelopes based on Tsai-Wu failure criteria, have been derived by IJsselmuiden et al.⁸ In this paper, omnistrain failure envelopes are generated numerically, instead. This numerical technique can deal with complex failure criteria which includes multiple modes of failure like Hashin failure criteria.

The rest of this paper is organized as follows: section Three dimensional failure Envelopes discusses the properties and the generation of the three dimensional failure envelopes. Section Omnistrain Failure Envelope Generation for Composite Materials proposes a numerical technique to generate the omnistrain failure envelopes from the three dimensional envelope. Section Results presents the resulted omnistrain envelopes based on Tsai-Wu, Hashin and Puck failure criteria. It also includes a comparison between both of the criteria and results from the literature. The results of the adaptive algorithm are also presented in this section. Section Conclusion discusses the conclusion of this paper.

Three dimensional failure envelopes

Three dimensional failure envelopes usually represented in material coordinates in terms of the critical stresses at failure (σ_1^c , σ_2^c and τ_{12}^c),

$$f(\sigma_1^c, \sigma_2^c, \tau_{12}^c) = 1 \quad (1)$$

The safe region is represented by the following inequality,

$$f(\sigma_1^c, \sigma_2^c, \tau_{12}^c) \leq 1 \quad (2)$$

Based on the factor of safety definition given in⁹, the failure envelope can be redefined,

$$f(\lambda\sigma_1, \lambda\sigma_2, \lambda\tau_{12}) = 1 \quad (3)$$

where, λ is the factor of safety which is function of the stresses (σ_1 , σ_2 and τ_{12}).

Omnistrain failure envelopes are defined in strain space mainly because the failure strains in fiber and matrix directions are comparable, while failure envelopes in stress space are highly elongated. Since the composites in general are brittle, a linear relationship can be assumed between stresses and strains to transform the previous expressions into strain space.

$$g(\lambda\epsilon_1, \lambda\epsilon_2, \lambda\gamma_{12}) = 1 \quad (4)$$

In the absence of a direct functional definition of the failure envelope, and with the assumption that the failure envelope is convex, a function called the failure index can be defined as shown in Figure 1 to be

$$r(\epsilon) = \frac{\overline{OP}}{\overline{OP'}} = \frac{1}{\lambda(\epsilon)} \quad (5)$$

It can be shown that the failure index is the inverse of the factor of safety defined in⁹ and is a convex function of strains as proved in appendix Convex Sets and Convex Functions

In order to sample the failure surface, a set of points ($\epsilon_1^s, \epsilon_2^s, \gamma_{12}^s$) are generated in the strain space that are not necessarily on the failure surface. For each point the failure index is calculated numerically depending on the failure criteria involved. By definition the inverse of the failure index multiplied by the strain generates a point on the failure surface,

$$\epsilon_1 = \frac{1}{r} \epsilon_1^s \quad \epsilon_2 = \frac{1}{r} \epsilon_2^s \quad \gamma_{12} = \frac{1}{r} \gamma_{12}^s \quad (6)$$

where ($\epsilon_1, \epsilon_2, \gamma_{12}$) is a point on the failure surface. In this way, a set of points on the failure surface are generated. Then, Qhull algorithm¹⁰ is used to generate a polygonal approximation of the surface as shown in Figure 1(b).

The failure criteria may be defined by more than one function as in Hashin failure criterion.³ In this case the failure index is calculated for each function, then the maximum failure index is used. The maximum of multiple failure indices represents the most critical inner intersection of multiple envelopes.

Omnistrain failure envelope generation for composite materials

In the previous section, a convex hull is obtained as an approximation of the failure surface. Convex hull is defined to be the smallest convex enclosure containing a set of points. Each facet of the convex hull is simply a plane with the safe region being a halfspace. The halfspaces of all planes (forming the convex hull) are represented by a set of linear inequalities in the strain space.

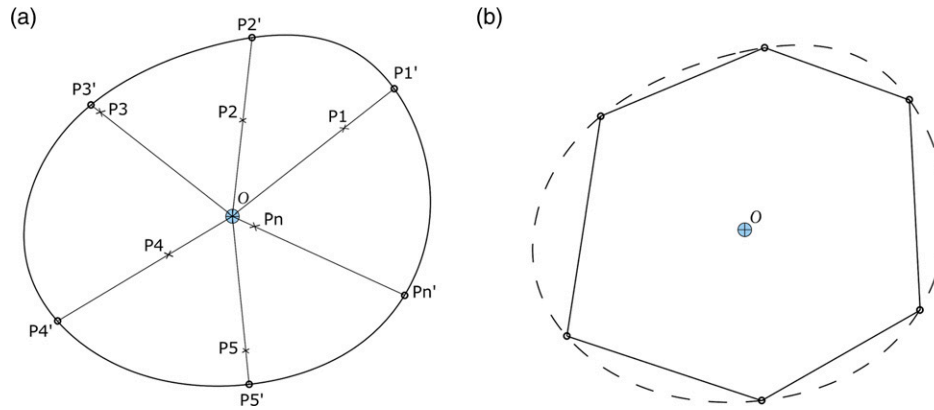


Figure 1. Generation of the failure surface from a set of arbitrary points in the strain space. (a) Sampled points of the failure surface. (b) Polygonal approximation of the failure surface.

$$\begin{aligned} l_1 \epsilon_1 + m_1 \epsilon_2 + n_1 \gamma_{12} &\leq c_1 \\ l_2 \epsilon_1 + m_2 \epsilon_2 + n_2 \gamma_{12} &\leq c_2 \\ &\vdots \\ l_M \epsilon_1 + m_M \epsilon_2 + n_M \gamma_{12} &\leq c_M \end{aligned} \quad (7)$$

Strains generated in the previous section were in material coordinates which can be transformed into principal coordinates through the following relations,

$$\begin{aligned} \epsilon_1 &= \epsilon'_1 \cos^2 \theta + \epsilon'_2 \sin^2 \theta \\ \epsilon_2 &= \epsilon'_1 \sin^2 \theta + \epsilon'_2 \cos^2 \theta \\ \gamma_{xy} &= (\epsilon'_1 - \epsilon'_2) 2 \sin \theta \cos \theta \end{aligned} \quad (8)$$

where θ is the angle between the principal and material coordinates. Substituting equation (8) into (7), a set of equations in the following form are obtained.

$$l_i (\epsilon'_1 \cos^2 \theta + \epsilon'_2 \sin^2 \theta) + m_i (\epsilon'_1 \sin^2 \theta + \epsilon'_2 \cos^2 \theta) + n_i ((\epsilon'_1 - \epsilon'_2) 2 \sin \theta \cos \theta) \leq c_i, i = 1 : M \quad (9)$$

where l_i , m_i , n_i and c_i are the coefficients of the equations of the halfspaces, then the following double angle relations will be used:

$$\begin{aligned} \cos^2 \theta &= \frac{1}{2} (1 + \cos 2\theta) \\ \sin^2 \theta &= \frac{1}{2} (1 - \cos 2\theta) \end{aligned} \quad (10)$$

leading to the following form of the inequality:

$$\begin{aligned} \left[\frac{(l_i - m_i)}{2} \cos 2\theta + n_i \sin 2\theta \right] (\epsilon_1 - \epsilon_2) + \\ \left(\frac{l_i + m_i}{2} \right) (\epsilon_1 + \epsilon_2) \leq c_i, i = 1 : M \end{aligned} \quad (11)$$

which could be rewritten in terms of volumetric strain ($\epsilon_v = \epsilon_1 + \epsilon_2$) and maximum shear strain ($\gamma_M = \epsilon_1 - \epsilon_2$) as follows:

$$\begin{aligned} \left[\frac{(l_i - m_i)}{2} \cos 2\theta + n_i \sin 2\theta \right] \gamma_M + \\ \left(\frac{l_i + m_i}{2} \right) \epsilon_v \leq c_i, i = 1 : M \end{aligned} \quad (12)$$

This equation represents a family of linear constraints in the plane $\epsilon_v - \gamma_M$ parameterized by the angle θ . Variation of the angle represents plies of different orientations at the stacking sequence of the composite. To obtain the omnistrain envelope, the most critical case—out of all the possible constraints—should be considered.

The critical constraint is obtained by maximizing the left hand side with respect to the angle θ . The coefficient of γ_M is harmonic in θ which means that its maximum is the amplitude. Now the most critical constraint is represented in the following form:

$$\left(\frac{l_i + m_i}{2} \right) \epsilon_v \pm \sqrt{\left(\frac{l_i - m_i}{2} \right)^2 + n_i^2} \gamma_M \leq c_i, i = 1 : M \quad (13)$$

The maximum shear strain γ_M can be positive or negative, thus a plus or minus sign is given to the amplitude term. The set of constraints defined by equation (13) represents a polygonal approximation of the omnistrain failure envelope.

Algorithm

- (1) Generate a set of arbitrary principal strains

$$\epsilon'_1 = \cos \psi, \quad \epsilon'_2 = \sin \psi, \quad \psi = \left[0 : \frac{2\pi}{M_1} : 2\pi \right] \quad (14)$$

where $2\pi/M_1$ is a fixed increment

- (2) All possible rotations of the generated principal strains are obtained using the following equation:

$$\begin{aligned}\epsilon_1 &= \epsilon'_1 \cos^2 \phi + \epsilon'_2 \sin^2 \phi \\ \epsilon_2 &= \epsilon'_1 \sin^2 \phi + \epsilon'_2 \cos^2 \phi \\ \gamma_{xy} &= (\epsilon'_1 - \epsilon'_2) 2 \sin \phi \cos \phi, \phi = \left[0 : \frac{\pi/2}{M_2} : \frac{\pi}{2} \right]\end{aligned}\quad (15)$$

where $(M = M_1 M_2)$ is the number of sampled strain points.

- For each strain point, the failure index is calculated and a point on the failure surface is defined by equation (6).
- In the presence of multiple failure modes as in example Hashin, the most critical failure index is the maximum.
- Using Qhull the convex hull is constructed from the set of strain points
- Qhull output is set to generate halfspace form resulting in a set of inequalities 7.
- Each halfspace is used to generate two constraints of the form 13. This set of constraints now represents the halfspace representation of the omnistrain envelope.
- Run Qhull over the intersections halfspaces to obtain the convex hull of the omnistrain envelope.

Adaptive algorithm

The accuracy of the omnistrain envelopes showed dependence on the number of sampling points. An adaptive algorithm is suggested to minimize the number of sampling points. The algorithm is based on starting with the least number of sampling points in the strain space and evaluating the corresponding points on the failure surface. The convex hull is then obtained as discussed before in section Algorithm. The convex hull consists of a set of triangles. Then, the centroid of each triangle is defined.

The failure index will be calculated for these centroids. Five percent of these centroids which have the lowest failure indices, will be chosen and added to the sampling points as shown in Figure 2.¹ The error is defined as follows:

$$e = (1 - \min\{r_{c_1}, r_{c_2}, r_{c_3}, \dots, r_{c_i}\}) 100 \quad (16)$$

The algorithm is repeated until a threshold on the error value is achieved.

Results

In this section, we consider the generation of omnistrain failure envelopes for the composite materials listed in Tables 1, 2 and 3.

Tsai-Wu failure criteria

The analytic expressions of the omnistrain failure envelopes of Tsai-Wu failure criterion are generated in.⁸ Incorporating these expressions into the algorithm stated in section Algorithm for a different number of sampling points, Figures 3, 4 and 5 are obtained.

In analytic expression based on the type of material, there exists two types of envelopes. One type is essentially an ellipse as shown in Figures 3(a) and 4(a). The other type is an intersection of two ellipses as in Figure 5(a). The previous results prove the robustness and the ability of the algorithm to track the envelope irrespective of the shape of the envelope. Additionally, they clearly show that fewer sampling points result in increasing error as shown in Figures 3(c), 4(c) and 5(c).

Adaptive algorithm

In this section, omnistrain failure envelopes are generated for Carbon Peek and Boron Epoxy using the

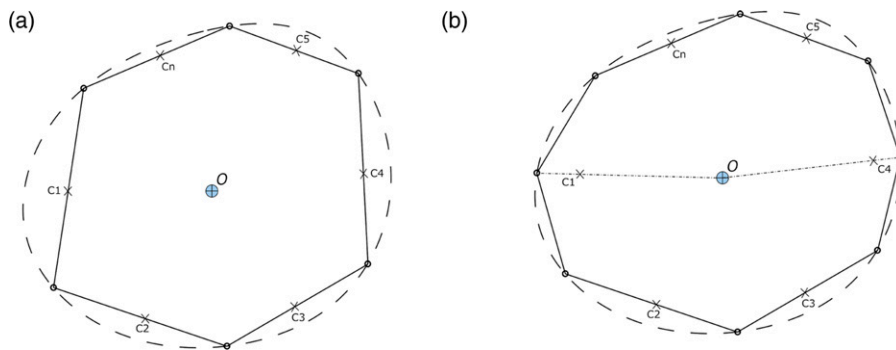


Figure 2. Application of the adaptive algorithm on the polygonal approximation of the failure surface. (a) Polygonal approximation of the failure surface. (b) Polygonal approximation of the failure surface after applying adaptive algorithm.

Table 1. Material properties.

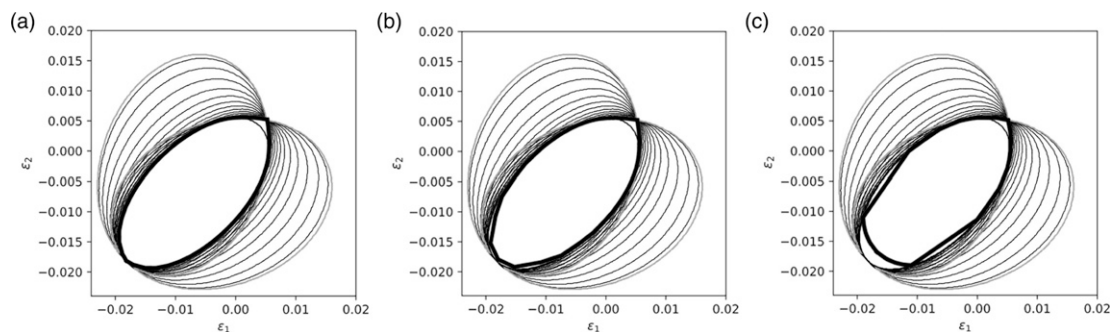
	Carbon/PEEK (AS4)	Carbon/epoxy (IM6)
Longitudinal modulus (E_1 , GPa)	142.0	177.0
Transverse modulus (E_2 , GPa)	10.3	10.8
Shear modulus (G_{12} , GPa)	7.2	7.6
Poisson's ratio (ν_{12})	0.27	0.27
Longitudinal tensile strength (X_t , MPa)	2280.0	2860.0
Longitudinal compressive strength (X_c , MPa)	1440.0	1875.0
Transverse tensile strength (Y_t , MPa)	57.0	49.0
Transverse compressive strength (Y_c , MPa)	228.0	246.0
Shear strength (S , MPa)	71.0	83.0

Table 2. Material properties.

	Boron/Epoxy (B5.6)	E-Glass/Epoxy
Longitudinal modulus (E_1 , GPa)	201.0	41.0
Transverse modulus (E_2 , GPa)	21.7	10.4
Shear modulus (G_{12} , GPa)	5.4	4.3
Poisson's ratio (ν_{12})	0.17	0.28
Longitudinal tensile strength (X_t , MPa)	1380.0	1140.0
Longitudinal compressive strength (X_c , MPa)	1600.0	620.0
Transverse tensile strength (Y_t , MPa)	56.6	39.0
Transverse compressive strength (Y_c , MPa)	125.0	128.0
Shear strength (S , MPa)	62.6	89.0

Table 3. Material properties.

	S-Glass/Epoxy
Longitudinal modulus (E_1 , GPa)	45.0
Transverse modulus (E_2 , GPa)	11.0
Shear modulus (G_{12} , GPa)	4.5
Poisson's ratio (ν_{12})	0.29
Longitudinal tensile strength (X_t , MPa)	1725.0
Longitudinal compressive strength (X_c , MPa)	690.0
Transverse tensile strength (Y_t , MPa)	49.0
Transverse compressive strength (Y_c , MPa)	158.0
Shear strength (S , MPa)	70.0

**Figure 3.** Carbon peek. (a) $M = 2500$ (b) $M = 625$ (c) $M = 144$. Tsai-Wu strain envelopes for $\theta = 0, 5, \dots, 90$ deg ———. Omnistrain envelope based on Tsai-Wu failure criteria ———.

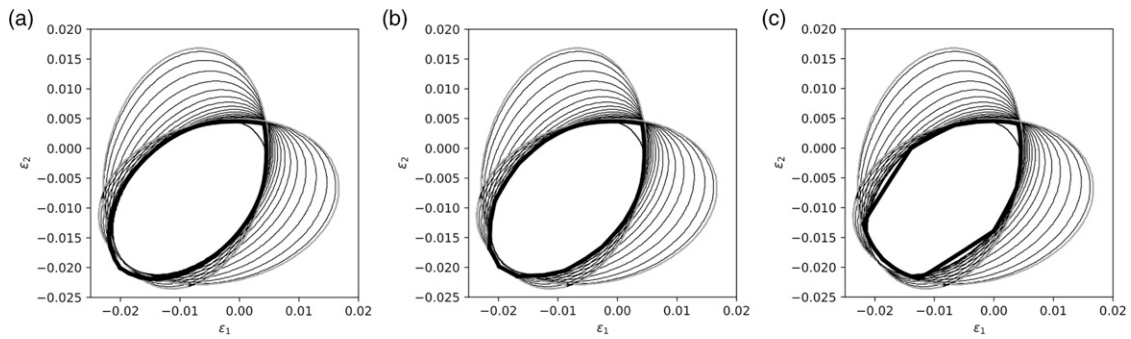


Figure 4. Carbon Epoxy. (a) $M = 2500$ (b) $M = 625$ (c) $M = 144$. Tsai-Wu strain envelopes for $\theta = 0, 5, \dots, 90$ deg ———. Omnistrain envelope based on Tsai-Wu failure criteria ———.

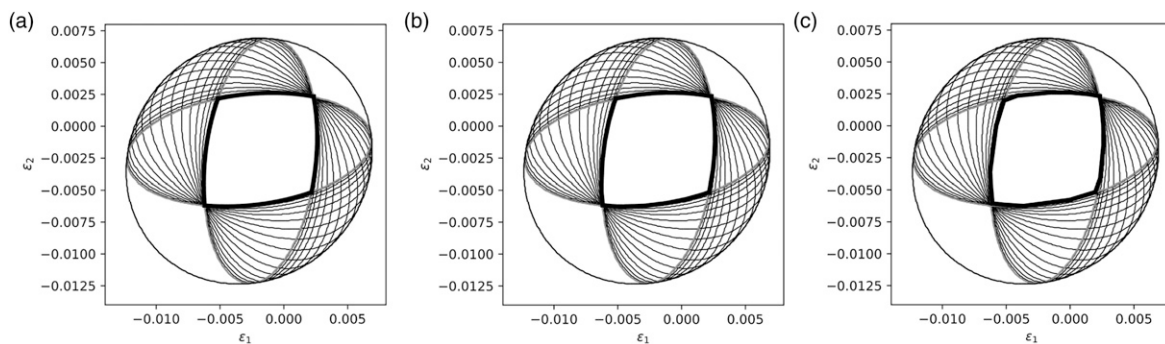


Figure 5. Boron Epoxy. (a) $M = 2500$ (b) $M = 625$ (c) $M = 144$. Tsai-Wu strain envelopes for $\theta = 0, 5, \dots, 90$ deg ———. Omnistrain envelope based on Tsai-Wu failure criteria ———.

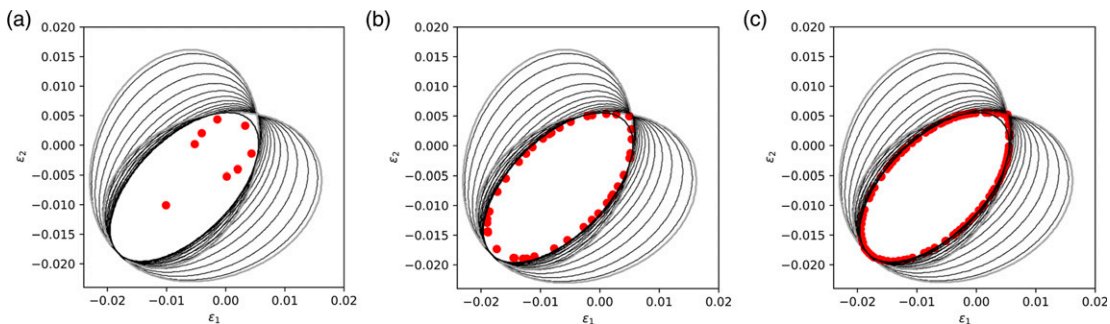


Figure 6. Adaptive algorithm results at different correction steps for Carbon Peek (a) Step 1, $M = 9$, Error = 61.45% (b) Step 21, $M = 72$, Error = 6.61% (c) Step 42, $M = 532$, Error = 0.94%.

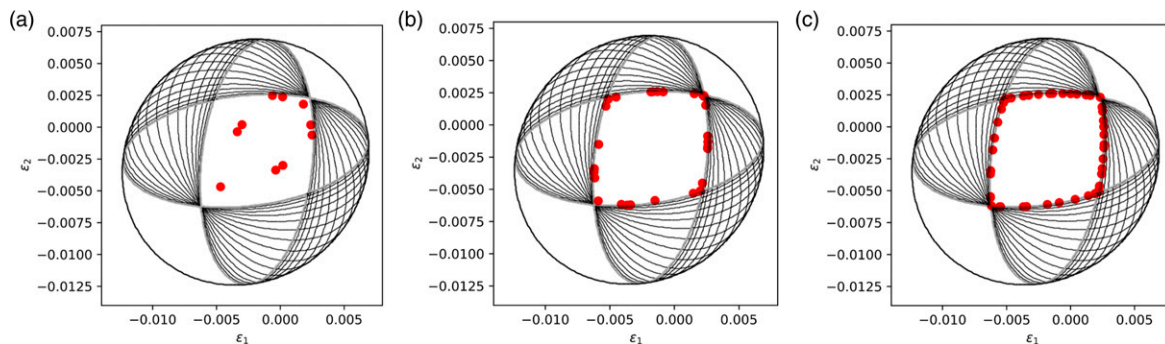


Figure 7. Adaptive algorithm results at different correction steps for Boron Epoxy (a) Step 1, $M = 9$, Error = 72.29% (b) Step 21, $M = 72$, Error = 6.46% (c) Step 41, $M = 493$, Error = 0.96%.

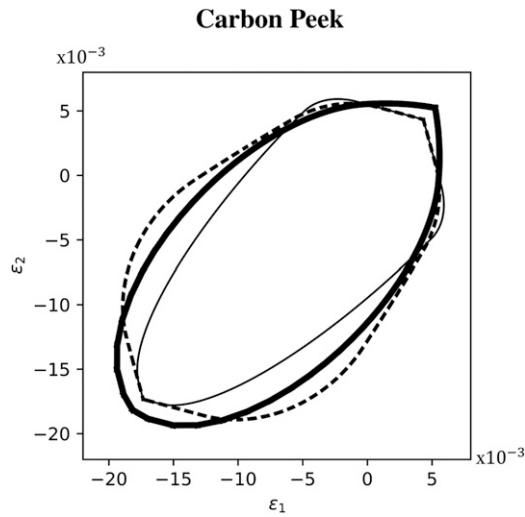


Figure 8. Comparison between different failure criteria (Hashin failure criteria —, Tsai-Wu failure criteria —, Puck failure criteria ---).

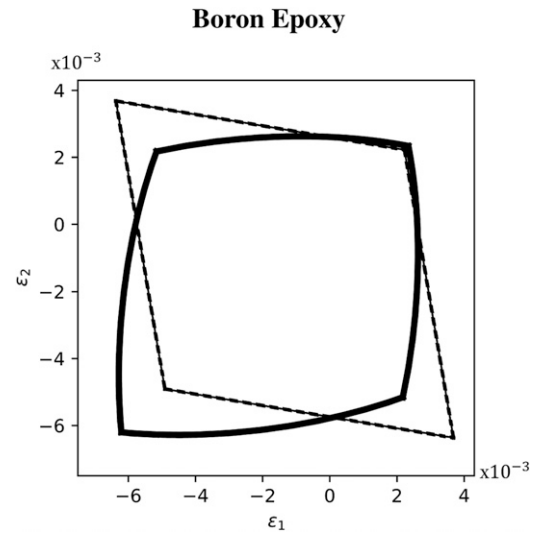


Figure 10. Comparison between different failure criteria (Hashin failure criteria —, Tsai-Wu failure criteria —, Puck failure criteria ---).

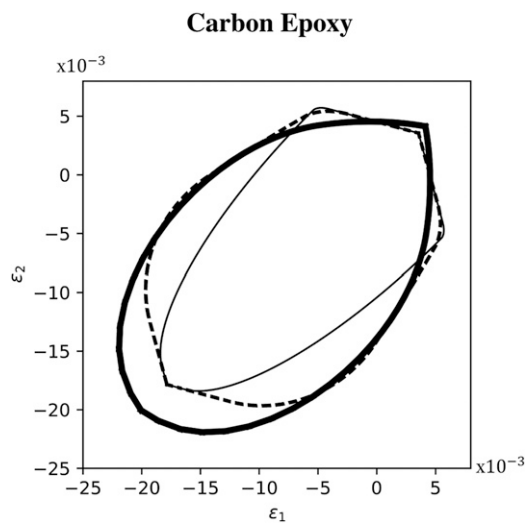


Figure 9. Comparison between different failure criteria (Hashin failure criteria —, Tsai-Wu failure criteria —, Puck failure criteria ---).

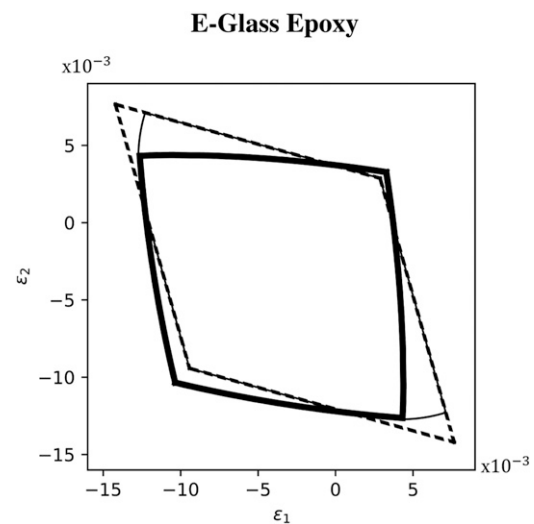


Figure 11. Comparison between different failure criteria (Hashin failure criteria —, Tsai-Wu failure criteria —, Puck failure criteria ---).

adaptive algorithm as shown in Figures 6 and 7. Clearly, Figures 6(c) and 7(c) exhibit results that are remarkably congruent with those depicted in Figures 3(a) and 4(a), respectively. This observation is noteworthy as Figures 6(c) and 7(c) were generated using a significantly reduced number of sampling points. The profound similarity between the two sets of results serves as a proof of the computational efficiency of the algorithm and its ability to achieve comparable

outcomes while operating with a reduced computational cost.

Comparison of different failure criteria

The analytic expressions derived in the appendices are used to generate the curves of Figures 8, 9, 10, 11 and 12.

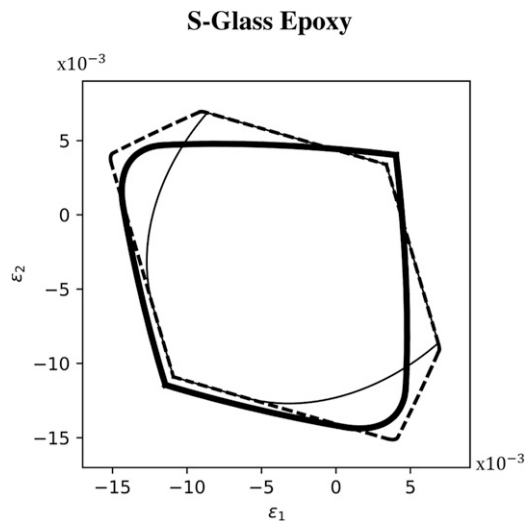


Figure 12. Comparison between different failure criteria (Hashin failure criteria —, Tsai-Wu failure criteria —, Puck failure criteria - - -).

It is clear that Hashin is more conservative than Tsai-Wu in the third quadrant which represents the compression-compression case.

Conclusion

Numerical generation of omnistrain failure envelopes based on different failure criteria is presented. Three dimensional failure surfaces are constructed as a polygonal approximation of sampled failure points in the strain space. Sampling the points of the three dimensional failure surface relies on calculating the failure index, which is proved to be a convex function, and does not require a functional description of the failure surface. As a result, omnistrain envelopes can be generated for any failure criteria including those that are not defined by a single analytical expression such as Hashin criteria. The number of sampling points highly affects the accuracy of the generated envelopes. Results based on Tsai-Wu failure criteria showed a great match with analytic expressions regardless the shape of the envelope. Comparison between Hashin criteria and Tsai-Wu criteria showed that Hashin criteria is more conservative in the third quadrant (compression-compression) and is very close to Tsai-Wu criteria in the other quadrants.

Discussion

This work presents a strain-based failure criterion. The developed omnistrain envelopes take advantage of the

invariance of failure envelopes in strain space. Hence, a master failure envelope can be developed for a laminate in strain space, regardless of the layup. Being expressed in terms of strain makes it more robust and universal as strains are almost constant at the onset of irreversible damage. Unlike stresses, which vary dramatically at failure, depending on deformation mode, strains are almost identical and independent of failure mode or the load type. Strains can also be easily measured through experiment and calculated using different laminate theories, rather than using arbitrary assumed parameters that were used for fitting envelopes on test data¹¹. Moreover, strains represent a physical meaning related to deformations.

The proposed methodology allows for evaluating the most critical omnistrain failure envelope by comparing different failure criteria as shown in Figures 8, 9, 10, 11 and 12. Additionally, it opens the door for using criteria that deal with composite materials as two discrete constituents (matrix and fiber), such as the Strain Invariant Failure Theory (SIFT)¹¹, where each constituent needs to be assessed for each failure mode independently. It is assumed that both kinds of deformation modes (distortion and dilatation) are coexisting. The focus should be on which mode will become critical first and in which constituent (fiber or matrix). Furthermore, the scope of this research can be extended to incorporate plasticity as in this work only brittle composites were considered. Moreover, an enhancement could be made by incorporating time-dependent failure criteria into the study.

Author's notes

In Memoriam: Dr. Mostafa Abdalla

This publication is dedicated to the memory of our esteemed coauthor, Dr. Mostafa Abdalla, who regrettably passed away on July 2023. Dr. Mostafa left an indelible mark on the field of composite materials and structural optimization. Dr. Mostafa's academic journey spanned continents, from Cairo University to Virginia Tech and Delft University of Technology, where he earned his PhD. Finally, he was a full professor at Zewail City of Science and Technology in Egypt, where he held the position of Head of the Department of Aerospace Engineering.

Dr. Mostafa was renowned for his pioneering contributions to the optimization of composite materials, particularly in the context of aerospace applications. His remarkable insights and ingenuity paved the way for revolutionary advancements in the design and manufacturing of composite structures. Notably, his work on optimizing fiber-steered laminates, which entail an intricate design space, remains invaluable to composite and aircraft manufacturers worldwide.

Beyond his remarkable scientific achievements, Dr. Mostafa's warm and inspiring personality touched the lives of his colleagues, students, and friends alike. His wisdom, patience, humanity, and kindness serve as a guiding light for all who had the privilege of knowing him.

This publication is a tribute to Dr. Mostafa Abdalla's enduring legacy, a legacy of innovation, generosity, and brilliance that will forever resonate in the field of composite materials. His legacy lives on through his publications and the enduring impact of his work. We fondly remember his contributions and the remarkable person he was.

Declaration of conflicting interests

The author(s) declared no potential conflicts of interest with respect to the research, authorship, and/or publication of this article.

Funding

The author(s) received no financial support for the research, authorship, and/or publication of this article.

ORCID iD

Mohamed H. Elalfy  <https://orcid.org/0000-0003-2135-2614>

Note

1. It is important to clarify that [Figures 1 and 2](#) represent two dimensional projection of the three dimensional convex hull.

References

1. Tsai SW. *Strength theories of filamentary structures*. Wiley Interscience, 1968, pp. 3–11.
2. Tsai SW and Wu EM. A general theory of strength for anisotropic materials. *J Compos Mater* 1971; 5(1): 58–80.
3. Hashin Z. *Fatigue failure criteria for unidirectional fiber composites*. Technical report Pennsylvania University Philadelphia Department of Materials Science and Engineering, 1980.
4. Tsai SW and Melo JDD. An invariant-based theory of composites. *Compos Sci Technol* 2014; 100: 237–243.
5. Tsai SW and Melo JDD. A unit circle failure criterion for carbon fiber reinforced polymer composites. *Compos Sci Technol* 2016; 123: 71–78.
6. Furtado C, Arteiro A, Bessa M, et al. Prediction of size effects in open-hole laminates using only the young's modulus, the strength, and the r-curve of the 0 ply. *Compos Appl Sci Manuf* 2017; 101: 306–317.
7. Millen SL and Aravand MA. Assessing the relative conservatism of the unit circle failure envelope. *Compos Commun* 2021; 24: 100690.
8. Ijsselmuiden ST, Abdalla MM and Gurdal Z. Implementation of strength-based failure criteria in the lamination parameter design space. *AIAA J* 2008; 46(7): 1826–1834.
9. Groenwold AA and Haftka RT. Optimization with non-homogeneous failure criteria like Tsai–Wu for composite laminates. *Struct Multidiscip Optim* 2006; 32(3): 183–190.
10. Barber CB, Dobkin DP and Huhdanpaa H. *Qhull: Quickhull algorithm for computing the convex hull*. Astrophysics Source Code Library, 2013. ascl - 1304.
11. Hart-Smith L. Application of the strain invariant failure theory (sift) to metals and fiber–polymer composites. *Phil Mag* 2010; 90(31–32): 4263–4331.
12. Puck A and Schurmann H. Failure analysis of frp laminates by means of physically based phenomenological models. *Compos Sci Technol* 2002; 62(12–13): 1633–1662.
13. Puck A and Schurmann H. Failure analysis of frp laminates by means of physically based phenomenological models. *Failure criteria in fibre-reinforced-polymer composites*. Amsterdam: Elsevier, 2004, pp. 832–876.
14. Puck A and Mannigel M. Physically based non-linear stress–strain relations for the inter-fibre fracture analysis of frp laminates. *Compos Sci Technol* 2007; 67(9): 1955–1964.

Appendices

Convex Sets and Convex Functions

A closed set \mathbb{C} is convex at the following condition:

$$\forall x_1, x_1 \in \mathbb{C} \Rightarrow (1 - \alpha)x_1 + \alpha x_2 \in \mathbb{C}, \alpha \in [0, 1] \quad (17)$$

A function $f(x)$ is convex if the following condition is attained:

$$f((1 - \alpha)x_1 + \alpha x_2) \leq (1 - \alpha)f(x_1) + \alpha f(x_2) \quad (18)$$

Failure envelopes define a space of safe loading which is observed to be a convex set. An arbitrary point P in the safe space can be related to another point P' , on the failure surface and along the line connecting P to the origin O , as follows:

$$\frac{\overline{OP'}}{\overline{OP}} = \lambda(\varepsilon) \quad (19)$$

Another function which is well-behaving near the origin, unlike $\lambda(\varepsilon)$, is called the failure index and is defined as follows:

$$r(\varepsilon) = \frac{1}{\lambda(\varepsilon)} = \frac{\overline{OP}}{\overline{OP'}} \quad (20)$$

Proposition 1. $r(\varepsilon)$ is a convex function over \mathbb{C}

Proposition 2. $r(\varepsilon)$ is homogeneous function of order 1

Tsai-Wu Criterion

Tsai-Wu failure criterion² was an improvement of Tsai-Hill. In order to get a better match with the experimental data, the number of terms in the prediction equation need to

be increased. In tensor form the criterion is defined as follows,

$$F_i \sigma_i + F_{ij} \sigma_i \sigma_j = 1 \quad i, j = 1, \dots, 6 \quad (21)$$

where F_i is second order tensor and F_{ij} is fourth order tensor, both representing strength parameters. Being expressed in tensorial form, added a great advantage and flexibility to the criterion. The criterion is invariant under rotation and obeys tensor transformation which made analysis easier.

In case of an orthotropic lamina under plane stress conditions, equation (21) reduces to the following form,

$$F_1 \sigma_1 + F_2 \sigma_2 + F_{11} \sigma_1^2 + F_{22} \sigma_2^2 + 2F_{12} \sigma_1 \sigma_2 + F_{66} \tau_{12}^2 = 1 \quad (22)$$

where,

$$F_1 = \frac{1}{X_c} + \frac{1}{X_t}, F_2 = \frac{1}{Y_c} + \frac{1}{Y_t}, F_{11} = \frac{-1}{X_c X_t},$$

$$F_{22} = \frac{-1}{Y_c Y_t}, F_{66} = \frac{1}{S^2}, F_{12} = \frac{-1}{2\sqrt{X_t X_c Y_t Y_c}}$$

For an arbitrary point in the strain plane (ϵ_1 , ϵ_2 and γ_{12}), the corresponding point on the failure envelope is defined by first calculating the stresses through stress-strain relation:

$$\begin{bmatrix} \sigma_1 \\ \sigma_2 \\ \tau_{12} \end{bmatrix} = \begin{bmatrix} Q_{11} & Q_{12} & 0 \\ Q_{12} & Q_{22} & 0 \\ 0 & 0 & Q_{66} \end{bmatrix} \begin{bmatrix} \epsilon_1 \\ \epsilon_2 \\ \gamma_{12} \end{bmatrix} \quad (23)$$

where the Q_{ij} are the reduced stiffnesses for a plane stress state and they are defined from material properties. The stresses are then scaled to their critical values using the safety factor and substituted in equation (22):

$$F_1 \lambda \sigma_1 + F_2 \lambda \sigma_2 + F_{11} \lambda^2 \sigma_1^2 + F_{22} \lambda^2 \sigma_2^2 + 2F_{12} \lambda^2 \sigma_1 \sigma_2 + F_{66} \lambda^2 \tau_{12}^2 = 1 \quad (24)$$

Since the previous expression is quadratic in λ , two solutions are obtained for the safety factor which corresponds to two values of failure indices:

$$\lambda^2 \underbrace{(F_{11} \sigma_1^2 + F_{22} \sigma_2^2 + 2F_{12} \sigma_1 \sigma_2 + F_{66} \tau_{12}^2)}_a + \underbrace{\lambda(F_1 \sigma_1 + F_2 \sigma_2)}_b \underbrace{-1}_c = 0 \quad (25)$$

$$\lambda_{1,2} = \frac{-b \pm \sqrt{b^2 - 4ac}}{2a} \Rightarrow r_{1,2} = \frac{2a}{-b \pm \sqrt{b^2 - 4ac}} \quad (26)$$

The critical failure index at this point, which is the maximum of the two values, is used to define a point on the failure envelope using equation (6). The procedure explained in section Omnistrain Failure Envelope Generation

for Composite Materials is then followed to generate the omnistrain failure envelope using Tsai-Wu failure criterion.

Hashin Criterion

Hashin³ proposed to separate matrix failure modes from those of the fiber. For each failure mode or mechanism, tension is distinguished from compression resulting in four distinct failure modes. Stress interactions in each failure mode are expressed in terms of quadratic polynomials as follows,

$$\text{Tensile Fiber Failure Mode: } \left(\frac{\sigma_1}{X_t}\right)^2 + \left(\frac{\tau_{12}}{S}\right)^2 \geq 1 \quad (27)$$

$$\text{Compressive Fiber Failure Mode: } \frac{-\sigma_1}{X_c} \leq 1 \quad (28)$$

$$\text{Tensile Matrix Failure Mode: } \left(\frac{\sigma_2}{Y_t}\right)^2 + \left(\frac{\tau_{12}}{S}\right)^2 \geq 1 \quad (29)$$

$$\text{Compressive Matrix Failure Mode: } \left(\frac{\sigma_2}{Y_c}\right)^2 + \left(\frac{\tau_{12}}{S}\right)^2 \geq 1 \quad (30)$$

The inequality constraints will become equality constraints when substituting with the critical stresses:

$$\left(\frac{\lambda \sigma_1}{X_t}\right)^2 + \left(\frac{\lambda \tau_{12}}{S}\right)^2 = 1 \rightarrow \lambda = \frac{1}{\sqrt{\left(\frac{\sigma_1}{X_t}\right)^2 + \left(\frac{\tau_{12}}{S}\right)^2}} \quad (31)$$

$$\rightarrow r = \sqrt{\left(\frac{\sigma_1}{X_t}\right)^2 + \left(\frac{\tau_{12}}{S}\right)^2}$$

$$\frac{-\lambda \sigma_1}{X_c} = 1 \rightarrow \lambda = \frac{-X_c}{\sigma_1} \rightarrow r = \frac{\sigma_1}{-X_c} \quad (32)$$

$$\left(\frac{\lambda \sigma_2}{Y_t}\right)^2 + \left(\frac{\lambda \tau_{12}}{S}\right)^2 = 1 \rightarrow \lambda = \frac{1}{\sqrt{\left(\frac{\sigma_2}{Y_t}\right)^2 + \left(\frac{\tau_{12}}{S}\right)^2}} \quad (33)$$

$$\rightarrow r = \sqrt{\left(\frac{\sigma_2}{Y_t}\right)^2 + \left(\frac{\tau_{12}}{S}\right)^2}$$

$$\begin{aligned} \left(\frac{\lambda\sigma_2}{Y_c}\right)^2 + \left(\frac{\lambda\tau_{12}}{S}\right)^2 &= 1 \rightarrow \lambda = \frac{1}{\sqrt{\left(\frac{\sigma_2}{Y_c}\right)^2 + \left(\frac{\tau_{12}}{S}\right)^2}} \\ \rightarrow r &= \sqrt{\left(\frac{\sigma_2}{Y_c}\right)^2 + \left(\frac{\tau_{12}}{S}\right)^2} \end{aligned} \quad (34)$$

Now for each strain combination, the corresponding stress values meet only two conditions from the previous condition. For example if $\sigma_1 \geq 0$ and $\sigma_2 \geq 0$, then equations (31) and (33) apply.

Puck's Criterion

Puck¹² developed his theory based on Hashin's work but with more physical foundation. Two independent failure criteria had been developed one for fiber fracture and the other for inter-fiber fracture (IFF). Puck assumed that fiber polymer structures behave in a brittle manner. The formulation was made for a rotating plane system called the fracture plane, at which the brittle fracture takes place. Three principal directions were defined to predict failure in different orientations. L and T are the in-plane longitudinal and transverse directions, while N is the normal out of plane direction.

The conditions for fiber failure (FF) were developed based on maximum strain criteria. With the addition of empirical coefficients, failure predictions came in a good agreement the experimental data. These conditions are formulated as follows,

Tensile FibCer Failure Mode:

$$\frac{1}{X_{\epsilon_1}} \left(\epsilon_1 + \frac{v_{f12}}{E_{f1}} m_{\sigma_f} \sigma_2 \right) \geq 1, \epsilon_1 + \frac{v_{f12}}{E_{f1}} m_{\sigma_f} \sigma_2 > 0 \quad (35)$$

Compressive Fiber Failure Mode:

$$\begin{aligned} \frac{1}{X_{\epsilon_c}} \left| \left(\epsilon_1 + \frac{v_{f12}}{E_{f1}} m_{\sigma_f} \sigma_2 \right) \right| + (10\gamma_{21})^2 &\geq 1, \\ \epsilon_1 + \frac{v_{f12}}{E_{f1}} m_{\sigma_f} \sigma_2 &\leq 0 \end{aligned} \quad (36)$$

Inter-fiber failure (IFF) conditions were developed based on the assumption that the composite behave in a very brittle manner at failure. The conditions are formulated as follows, Inter Failure Fiber - Mode A (Tensile Matrix Failure Mode):

$$\begin{aligned} \sqrt{\left(\frac{\tau_{12}}{S}\right)^2 + \left(1 - P_{\perp}^+ \frac{Y_t}{S}\right)^2 \left(\frac{\sigma_2}{Y_t}\right)^2} + P_{\perp}^+ \frac{\sigma_2}{S} \\ + \left| \frac{\sigma_1}{\sigma_{1D}} \right| \geq 1, \sigma_2 \geq 0 \end{aligned} \quad (37)$$

Inter Failure Fiber - Mode B (Compressive Matrix Failure Mode):

$$\begin{aligned} \frac{1}{S} \left(\sqrt{\tau_{12}^2 + (P_{\perp}^- \sigma_2)^2} + P_{\perp}^- \sigma_2 \right) + \left| \frac{\sigma_1}{\sigma_{1D}} \right| &\geq 1, \\ \sigma_2 < 0, 0 \leq \left| \frac{\sigma_2}{\tau_{12}} \right| &\leq \frac{R_{\perp\perp}^4}{|\tau_{21c}|} \end{aligned} \quad (38)$$

Inter Failure Fiber - Mode C (Compressive Matrix Failure Mode):

$$\begin{aligned} \left[\left(\frac{\tau_{12}}{2(1 + P_{\perp}^-)S} \right)^2 + \left(\frac{\sigma_2}{Y_c} \right)^2 \right] \frac{Y_c}{(-\sigma_2)} &\geq 1, \\ \sigma_2 < 0, 0 \leq \left| \frac{\tau_{12}}{\sigma_2} \right| &\leq \frac{|\tau_{21c}|}{R_{\perp\perp}^4} \end{aligned} \quad (39)$$

where m_{σ_f} is a mean magnification factor of the transverse stress for the fiber, p is the slope of the fracture envelope and σ_{1D} is an empirical stress value, determining the degradation of the fracture.

The inequality constraints will become equality constraints when substituting with the critical stresses:

Tensile Fiber Failure Mode:

$$\begin{aligned} \lambda \frac{\sigma_1}{X_t} + \lambda \left(v_{f12} \frac{E_1}{E_{f1}} \frac{m_{\sigma_f}}{X_t} - \frac{v_{12}}{X_t} \right) \sigma_2 &= 1 \\ \rightarrow \lambda &= \frac{1}{\frac{\sigma_1}{X_t} + \left(v_{f12} \frac{E_1}{E_{f1}} \frac{m_{\sigma_f}}{X_t} - \frac{v_{12}}{X_t} \right) \sigma_2} \\ \rightarrow r &= \frac{\sigma_1}{X_t} + \left(v_{f12} \frac{E_1}{E_{f1}} \frac{m_{\sigma_f}}{X_t} - \frac{v_{12}}{X_t} \right) \sigma_2 \end{aligned} \quad (40)$$

Compressive Fiber Failure Mode:

$$\begin{aligned} \frac{1}{X_c} \left| \lambda \left[\frac{\sigma_1}{E_1} + \left(\frac{E_1}{E_{f1}} v_{f12} m_{\sigma_f} - v_{12} \right) \sigma_2 \right] \right| \\ + \frac{100}{G_{12}^2} \lambda^2 \tau_{12}^2 = 1 \\ \underbrace{\lambda^2 \left(\frac{100\tau_{12}^2}{G_{12}^2} \right)}_a + \underbrace{\lambda \left| \frac{\sigma_1}{E_1} + \left(\frac{E_1}{E_{f1}} v_{f12} m_{\sigma_f} - v_{12} \right) \sigma_2 \right|}_{b} \underbrace{-1}_c = 0 \end{aligned}$$

$$\lambda = \max \left\{ \frac{-b + \sqrt{b^2 - 4ac}}{2a}, \frac{-b - \sqrt{b^2 - 4ac}}{2a} \right\}, \quad (41)$$

$$\rightarrow r = \frac{1}{\lambda}$$

Inter Failure Fiber - Mode A (Tensile Matrix Failure Mode):

$$\sqrt{\left(\lambda^2 \frac{\tau_{12}}{S}\right)^2 + \left(1 - P_{\perp\parallel}^+ \frac{Y_t}{S}\right)^2 \lambda^2 \left(\frac{\sigma_2}{Y_t}\right)^2} + P_{\perp\parallel}^+ \lambda \frac{\sigma_2}{S} = 1$$

$$\lambda = \frac{1}{\sqrt{\left(\frac{\tau_{12}}{S}\right)^2 + \left(1 - P_{\perp\parallel}^+ \frac{Y_t}{S}\right)^2 \left(\frac{\sigma_2}{Y_t}\right)^2} + P_{\perp\parallel}^+ \frac{\sigma_2}{S}}$$

$$r = \sqrt{\left(\frac{\tau_{12}}{S}\right)^2 + \left(1 - P_{\perp\parallel}^+ \frac{Y_t}{S}\right)^2 \left(\frac{\sigma_2}{Y_t}\right)^2} + P_{\perp\parallel}^+ \frac{\sigma_2}{S} \quad (42)$$

Inter Failure Fiber - Mode B (Compressive Matrix Failure Mode):

$$\frac{1}{S} \left(\sqrt{\lambda^2 \tau_{12}^2 + \lambda^2 (P_{\perp\parallel}^- \sigma_2)^2} + \lambda P_{\perp\parallel}^- \sigma_2 \right) = 1$$

$$\lambda = \frac{S}{\left(\sqrt{\tau_{12}^2 + (P_{\perp\parallel}^- \sigma_2)^2} + P_{\perp\parallel}^- \sigma_2 \right)}$$

$$r = \frac{\left(\sqrt{\tau_{12}^2 + (P_{\perp\parallel}^- \sigma_2)^2} + P_{\perp\parallel}^- \sigma_2 \right)}{S} \quad (43)$$

Inter Failure Fiber - Mode C (Compressive Matrix Failure Mode):

$$\left[\lambda^2 \left(\frac{\tau_{12}}{2(1 + P_{\perp\perp}^-)S} \right)^2 + \lambda^2 \left(\frac{\sigma_2}{Y_c} \right)^2 \right] \frac{Y_c}{(-\lambda \sigma_2)} = 1$$

$$\lambda = \frac{-\sigma_2}{Y_c \left[\left(\frac{\tau_{12}}{2(1 + P_{\perp\perp}^-)S} \right)^2 + \left(\frac{\sigma_2}{Y_c} \right)^2 \right]}$$

$$r = \frac{-Y_c}{\sigma_2} \left[\left(\frac{\tau_{12}}{2(1 + P_{\perp\perp}^-)S} \right)^2 + \left(\frac{\sigma_2}{Y_c} \right)^2 \right] \quad (44)$$

Empirical parameters estimation

The meaning magnification factor is estimated in¹³ to be as follows:

Reinforcement Type	m_{sf}
Glass fiber/epoxy	1.3
Carbon fiber/epoxy	1.1

(45)

Based on¹⁴ the recommended values of the slopes of the fracture envelopes are as follows:

Reinforcement Type	$p_{\perp\parallel}^{(-)}$	$p_{\perp\parallel}^{(+)}$
Glass Fiber	0.25	0.3
Carbon Fiber	0.3	0.35

(46)

More relationships are derived in¹³ relating parameters:

$$P_{\perp\perp}^- = P_{\perp\parallel}^- \frac{R_{\perp\perp}^A}{S} \quad (47)$$

$$R_{\perp\perp}^A = \frac{S}{2P_{\perp\parallel}^-} \left(\sqrt{1 + 2P_{\perp\parallel}^- \frac{Y_c}{S}} - 1 \right) \quad (48)$$

$$\tau_{21c} = S \sqrt{1 + 2P_{\perp\perp}^-} \quad (49)$$

The degradation effect is very small so it can be neglected as concluded in¹³. Regarding Boron the same empirical parameters of Carbon will be used since no data exist in literature.